

Coordination of Lewis Acid to η^2 -Enonepalladium(0) Leading to Continuous Structure Variation from η^2 -Olefin Type to η^3 -Allyl Type

Sensuke Ogoshi,* Tomohiro Yoshida, Takuma Nishida, Masaki Morita, and Hideo Kurosawa*

Contribution from the Department of Applied Chemistry, Faculty of Engineering, Osaka University, Suita, Osaka 565-0871, Japan

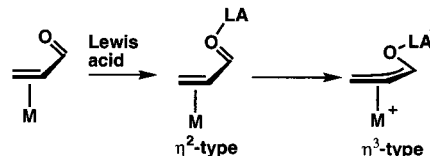
Received October 6, 2000

Abstract: The reaction of α,β -unsaturated carbonyl compounds, a palladium(0) complex, and Lewis acids led to the formation of a new class of complexes showing a wide variety of structures with η^2 -type and η^3 -type coordination of the carbonyl compounds. The reaction of Pd(PhCH=CHCOCH₃)(PPh₃)₂ with BF₃·OEt₂ or B(C₆F₅)₃ quantitatively gave palladium complexes **1a,b** having BX₃-coordinated η^2 -enonepalladium structure, as revealed by X-ray structure analysis of the B(C₆F₅)₃ adduct **1b**. On the other hand, the reaction of Pd-(PhCH=CHCHO)(PPh₃)₂ with BF₃·OEt₂ or B(C₆F₅)₃ gave distorted zwitterionic η^3 -allylpalladium complexes **3a,b**, where the Pd–carbonyl carbon distance in **3a** (2.413(4) Å) is much shorter than that (2.96(1) Å) in **1b**. The values of the P–P coupling constant and ¹³C chemical shift for carbonyl carbon are useful criteria for predicting how the η^3 -coordination mode contributes to the structure of the enone–palladium–Lewis acid system. Molecular orbital calculations on the series of model complexes suggest that orbital overlap in the highest occupied molecular orbital between the palladium and carbonyl carbon is enlarged by coordination of the Lewis acid to the carbonyl group. Palladium-catalyzed conjugate addition of R–M (R–M = AlMe₃, AlEt₃, ZnEt₂) and its plausible reaction path are also reported.

Introduction

The transition metal-catalyzed conjugate addition of various organometallic reagents, e.g., AlR₃, ZnR₂, Cp₂ZrRCl, InR₃, and BR₃, to α,β -unsaturated carbonyl compounds is a very fundamental and useful reaction in organic synthesis.¹ However, little is known about its reaction course except for a vague recognition that a key role is played by a Lewis acid at some stage of the reaction, where the source of the acid can be the organometallic reagents themselves or an intentionally added promoter. Some related but scattered information led us to propose a general scheme in which Lewis acids coordinate first to oxygen of the enone ligand which is η^2 -bound to metal (Scheme 1). The η^2 -bound complex then undergoes intramolecular rearrangement to the η^3 -allyl intermediate which accompanies oxidation of the metal atom. For example, in the nickel-catalyzed conjugate addition of alkenyltin using chlorosilane as a promoter, η^3 -1-(siloxy)allylnickel(II) chloride was isolated as the key intermediate,² but it remains unclear what was the precursor of the η^3 -allyl complex. Theoretical studies on the conjugate addition of lithium organocuprate suggested that initial lithium cation

Scheme 1



coordination to oxygen of the η^2 -enonecopper(I) complex triggers the transformation.³ Our aim was to experimentally demonstrate the existence of a range of structures from the Lewis acid-coordinated η^2 -enone complex to the distorted η^3 -allyl (Scheme 1) to gain a deeper insight into the role of Lewis acids in transition metal-catalyzed conjugate addition. For this purpose, we chose a palladium system, since prior knowledge about the η^3 -allylpalladium complexes would help us to characterize this class of variable structural complexes. Moreover, the observation of the stoichiometric reactions would allow us to construct the mechanism of the palladium-catalyzed conjugate addition of alkylmetals.

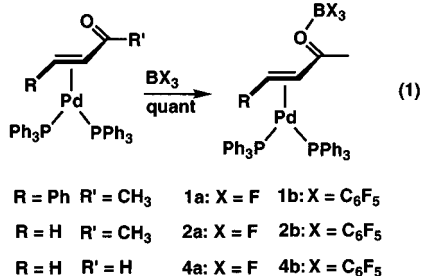
Results and Discussion

Synthesis and Structures. The reaction of the enone complex Pd(RCH=CHCOCH₃)(PPh₃)₂ with BF₃·OEt₂ or B(C₆F₅)₃ gave palladium complexes (R = Ph: **1a**, **1b**; R = H: **2a**, **2b**) quantitatively, having the expected composition in the elemental analysis (eq 1). The X-ray structure analysis of **1b** shows a

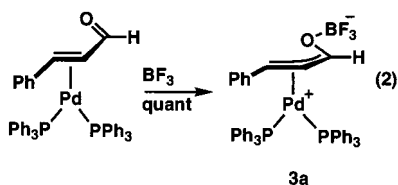
(2) Johnson, J. R.; Tully, P. S.; Mackenzie, P. B.; Sabat, M. *J. Am. Chem. Soc.* **1991**, *113*, 6172. Grisso, B. A.; Johnson, J. R.; Mackenzie, P. M. *J. Am. Chem. Soc.* **1992**, *114*, 5160.

(3) Nakamura, E.; Yamanaka, M. *J. Am. Chem. Soc.* **1999**, *121*, 8941. Nakamura, E.; Mori, S.; Morokuma, K. *J. Am. Chem. Soc.* **1997**, *119*, 4900.

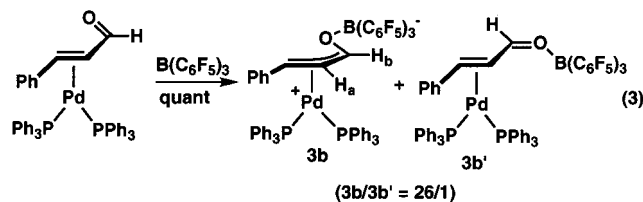
(1) Al: (a) Bagnell, L.; Jeffery, E. A.; Meisters, A.; Mole, T. *Aust. J. Chem.* **1975**, *28*, 801. (b) Hansen, R. T.; Carr, D. B.; Schwartz, J. *J. Am. Chem. Soc.* **1978**, *100*, 2244. (c) Schwartz, J.; Carr, D. B.; Hansen, R. T.; Dayrit, F. M. *J. Am. Chem. Soc.* **1980**, *102*, 3053. Zr: (d) Schwartz, J.; Loots, M. J.; Kosugi, H. *J. Am. Chem. Soc.* **1980**, *102*, 1333. (e) Hanzawa, Y.; Tabuchi, N.; Taguchi, T. *Tetrahedron Lett.* **1998**, *39*, 8141. Zn: (f) Greene, A. E.; Lansard, J.-P.; Luche, J.-L.; Petrier, C. *J. Org. Chem.* **1984**, *49*, 931. (g) Soai, K.; Hayasaka, T.; Ugajin, S. *J. Chem. Soc., Chem. Commun.* **1989**, 516. (h) Ikeda, S.-i.; Yamamoto, H.; Kondo, K.; Sato, Y. *Organometallics* **1995**, *14*, 5015. In: (i) Pérez, I.; Sestelo, J. P.; Maestro, M. A.; Sarandeses, L. A. *J. Org. Chem.* **1998**, *63*, 10074. B: (j) Cho, C. S.; Motofusa, S.-i.; Ohe, K.; Uemura, S. *J. Org. Chem.* **1995**, *60*, 883. (k) Takaya, Y.; Ogasawara, M.; Hayashi, T.; Sakai, M.; Miyaura, N. *J. Am. Chem. Soc.* **1998**, *120*, 5579.



B(C₆F₅)₃-coordinated η^2 -enonepalladium structure (Figure 1), in which the Pd–C3 distance (2.96(1) Å) is very close to the corresponding distance (2.91(2) Å) in the acid-free η^2 -enone complex Pt(PhCH=CHCOCH₃)(PPh₃)₂.⁴ The η^2 -enone bonding in **1a**, **2a**, and **2b** is deduced from NMR data, as will be discussed later. On the other hand, the reaction of the enal complex Pd(PhCH=CHCHO)(PPh₃)₂ with BF₃·OEt₂ gave a zwitterionic distorted η^3 -allylpalladium complex (**3a**), in which the Pd–C3 distance (2.413(4) Å) is much shorter than that (2.89–(2) Å) in Pt(PhCH=CHCHO)(PPh₃)₂ (eq 2, Figure 2).⁴ The



structure of **3a** represents another example of a distorted η^3 -allylpalladium complex,⁵ which is receiving increasing interest as a key structure in regioselective nucleophilic attack at η^3 -allylpalladiums. The reaction of Pd(PhCH=CHCHO)(PPh₃)₂ with B(C₆F₅)₃ gave the complex as a mixture of two isomers in solution (**3b**/**3b'** = 26/1) (eq 3). NOE measurements on the



major isomer **3b** show a strong interaction between H_a and H_b, as indicated in eq 3. The η^3 -allyl bonding in **3b** is deduced from NMR data, as will also be discussed later. However, the X-ray structure analysis of single crystals obtained from a solution of the mixture shows a B(C₆F₅)₃-coordinated η^2 -enonepalladium structure with s-trans configuration, **3b'** (Figure 3), which might correspond to the minor isomer in solution. It is of further interest that complexes **4a** and **4b** prepared from the reaction of Pd(CH₂=CHCHO)(PPh₃)₂ with BF₃·OEt₂ and B(C₆F₅)₃ have a structure intermediate between those of the η^2 -type and the η^3 -type complexes. The Pd–C3 distances in **4a** and **4b** are 2.59–(1) and 2.596(5) Å respectively.

In all those complexes analyzed crystallographically (**1b**, **3a**, **4a**, **4b**), Pd, C1, C2, P1, and P2 are on the same plane,⁶ and the torsion angle (Pd–C1–C2–C3) decreases as the Pd–C3

(4) Chaloner, P. A.; Davies, S. E.; Hitchcock, P. B. *Polyhedron* **1997**, *16*, 765.

(5) Togni, A.; Burckhardt, U.; Gramlich, V.; Pregosin, P. S.; Salzman, R. *J. Am. Chem. Soc.* **1996**, *118*, 1031. Burckhardt, U.; Gramlich, V.; Hofmann, P.; Nesper, R.; Pregosin, P. S.; Salzman, R.; Togni, A. *Organometallics* **1996**, *15*, 3496.

(6) The sum of the bond angles (deg) around Pd along the P1, P2, C1, and C2 atoms: **1b**, 361.1; **3a**, 359.7; **4a**, 359.9; **4b**, 358.3.

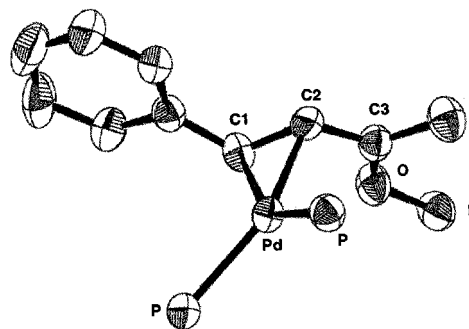


Figure 1. X-ray structure of **1b**. Selected bond lengths: Pd–C1 = 2.11(1) Å, Pd–C2 = 2.18(1) Å, Pd–C3 = 2.96(1) Å, C1–C2 = 1.45–(2) Å, C2–C3 = 1.41(2) Å, C3–O = 1.32(1) Å.

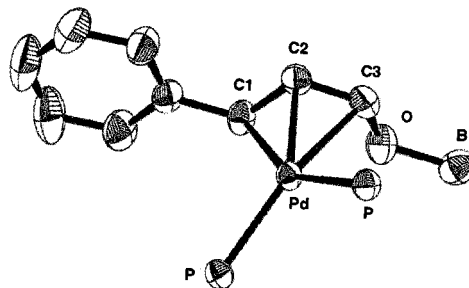


Figure 2. X-ray structure of **3a**. Selected bond lengths: Pd–C1 = 2.226(4) Å, Pd–C2 = 2.161(4) Å, Pd–C3 = 2.413(4) Å, C1–C2 = 1.416(5) Å, C2–C3 = 1.390(5) Å, C3–O = 1.309(5) Å.

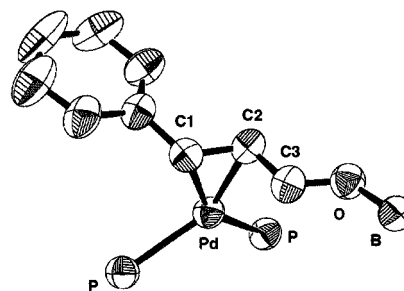


Figure 3. X-ray structure of **3b'**. Selected bond lengths: Pd–C1 = 2.10(1) Å, Pd–C2 = 2.117(1) Å, Pd–C3 = 2.65(1) Å, C1–C2 = 1.42–(2) Å, C2–C3 = 1.34(2) Å, C3–O = 1.31(2) Å.

Scheme 2



distance decreases (torsion angle (deg) for **1b**, 98(1)^o > **4b**, 80.9(4)^o > **4a**, 77.8(9)^o > **3a**, 71.4(3)^o).⁷ Thus, the structural change from η^2 to η^3 can be viewed as the rotation of the triangle defined by C1, C2, and C3 about the C1–C2 bond (Scheme 2).

The degree of the contribution of the η^3 -coordination mode to the structure in solution could also be evaluated from the ¹³C and ³¹P NMR data. The Pd–C3 distance, ¹³C chemical shift for carbonyl carbon, and P–P coupling constant for the complexes derived from the addition of BF₃·OEt₂ or B(C₆F₅)₃ to the enone complexes are summarized in Table 1. The

(7) Compared with the torsion angle (Pd–C1–C2–C3) and the Pd–C3 distance, other parameters including bond length (Pd–C1, Pd–C2, C1–C2, C2–C3, C3–O, O–B) and torsion angle (C2–C3–O–B) did not change so remarkably.

Table 1

	Pd–C3 (Å)	$\delta_{(\text{CO})}^a$	$J_{(\text{P-P})}^a$
1a		191.5	24.4
1b	2.96(1)	198.7	18.4
2a		187.2	19.5
2b		198.2	15.3
3a	2.413(4)	157.6	37.4
3b		166.0	30.5
4a	2.59(1)	161.5	29.4
4b	2.596(5)	169.7	25.7

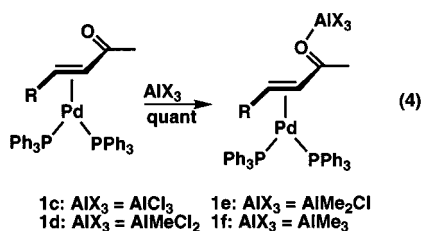
^a In C₆D₆.**Table 2**

	AIX ₃	Pd–C3 (Å)	$\delta_{(\text{CO})}^a$	$J_{(\text{P-P})}^a$
1c	AlCl ₃	2.61(1)	182.1	31.8
1d	AlMeCl ₂	2.649(6)	188.1	26.9
1e	AlMe ₂ Cl	2.69(1)	193.8	20.8
1f	AlMe ₃			13.5

^a In C₆D₆.

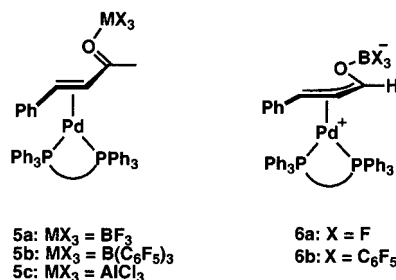
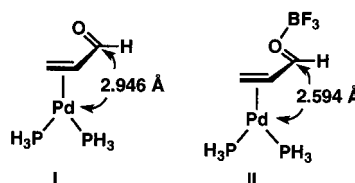
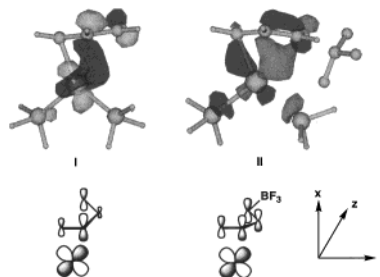
chemical shift of the carbonyl carbon at the higher magnetic field is correlated with the shorter Pd–C3 distance. A similar trend has been predicted by calculation for the cuprate–enone system.³ Moreover, the complex having the shorter Pd–C3 distance shows a P–P coupling constant closer to that (46.5 Hz) for $[(\eta^3\text{-PhCHCH}_2)\text{Pd}(\text{PPh}_3)_2]^+$. Thus, both values of the P–P coupling constant and ¹³C chemical shift for carbonyl carbon could be useful criteria for predicting how the η^3 -coordination mode contributes to the structure of the palladium–acid system. According to the criteria, the structure of the complexes without the X-ray structure analysis was classified as shown in eqs 1 and 3.

Similar treatment of Pd(PhCH=CHCOCH₃)(PPh₃)₂ with a series of aluminum compounds also led to the quantitative formation of the corresponding complexes **1c–f**, where the structures of **1c–e** were also determined. In this series, the criteria mentioned above can be applied as well (eq 4, Table 2). The orders of the upfield shifts of the carbonyl carbon



resonances and the P–P coupling constants are the same as that of the Lewis acidity (**1c** > **1d** > **1e** > **1f**), which indicates that stronger Lewis acid induces the η^3 -allyl structure to a greater extent. This is consistent with the small but steady decrease of the Pd–C3 distance in the order **1c** < **1d** < **1e**.

Similarly, 1,1'-bis(diphenylphosphino)ferrocene (DPPF)-coordinated complexes were also prepared (Scheme 3). Reaction of the (PhCH=CHCOCH₃)Pd(dppf) complex with BF₃, B(C₆F₅)₃, and AlCl₃ gave the corresponding complexes, **5a–c**. X-ray structure analyses on **5b** and **5c** indicate that each Pd–C3 distance (2.875(5), 2.56(2) Å) is slightly shorter than that in the corresponding bistrisphenylphosphine complex (**1b** and **1c**), respectively. More importantly, AlCl₃ makes a greater contribution to the η^3 -allyl form than B(C₆F₅)₃ (compare **5c** vs **5b**, and **1c** vs **1b**). The reaction of (PhCH=CHCHO)Pd(dppf) with BF₃ or B(C₆F₅)₃ also gave the corresponding complexes **6a,b**, where

Scheme 3**Scheme 4****Scheme 5**

J_{PP} (**6a**, 54.4 Hz; **6b**, 51.4 Hz) of the complex derived from enal is again larger than that in the complex derived from enone (**5a**, 45.9 Hz; **5b**, 41.9 Hz).

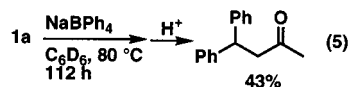
MO Calculation of the Model Complexes. To understand how the coordination of Lewis acids contributes to changing the coordination mode of enone ligand, B3LYP geometry optimizations were performed on model complexes, i.e., η^2 -acrolein complex **I** and BF₃ coordination complex **II** (Scheme 4). Palladium–carbon distances in the optimized geometry of **II** (Pd–C1 2.195 Å, Pd–C2 2.233 Å, Pd–C3 2.594 Å) show nice correlation to the experimental data (**4a**, Pd–C1 2.094(9) Å, Pd–C2 2.151(9) Å, Pd–C3 2.59(1) Å; **4b**, Pd–C1 2.161(5) Å, Pd–C2 2.145(5) Å, Pd–C3 2.596(5) Å). For comparison, in **I**, Pd–C1, Pd–C2, and Pd–C3 are 2.167, 2.203, and 2.946 Å, respectively. The calculations also showed that the atoms Pd, C1, C2, and P1 and P2 are on the same plane.⁸ From these results, it may reasonably be concluded that the B3LYP optimization can reproduce well the characteristic features of the bonding interaction between enone ligand, Lewis acid, and Pd(PH₃)₂.

Ab initio MO/MP2 calculations were performed on the optimized geometry of **I** and **II** (Scheme 5). The highest occupied molecular orbital (HOMO) of **I** shows no interaction between d_{xy} and p_x of carbonyl carbon. On the other hand, coordination of BF₃ enlarges the contribution of p_x on the carbonyl carbon in the HOMO of **II** to increase the interaction between Pd d_{xy} and carbonyl carbon, which shortens the Pd–C3 distance due to the electron donation (back-donation) from Pd to carbonyl carbon. In other words, more positive carbonyl carbon shortens the Pd–C3 distance and increases the oxidation

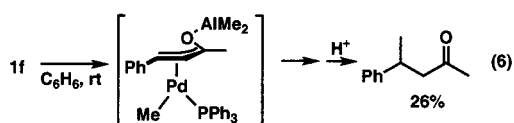
(8) The sums of the bond angles (deg) around Pd along P1, P2, C1, and C2 atoms are, for **I**, 360.0, and for **II**, 360.6.

state of Pd more. In fact, natural bond orbital (NBO) population analysis indicates that the Pd atomic charge in model complex **II** (0.237) is more positive than that in **I** (0.120) and approaches that in $[(\eta^3\text{-allyl})\text{Pd}(\text{PPh}_3)_2]^+$ (0.307).⁹ Such a greater positive charge of palladium in **II** due to the coordination of a Lewis acid has a significant implication in considering the transmetalation step for the conjugate addition, as will be discussed in more detail below. Moreover, this idea nicely accounts for the observations described above: (1) the Pd–C3 distance in **1b** is longer than that in **3a**, since the positive charge in **1b** could be delocalized by the attached CH₃ group; (2) there is a steady decrease of the Pd–C3 distance in the order **1c** < **1d** < **1e**, since a stronger Lewis acid can generate a larger positive charge on the carbonyl carbon.

Stoichiometric Reaction with NaBPh₄. In the palladium-catalyzed addition of organozirconium^{1c} and organoboron^{1g} to enones, Lewis acids including BF₃ are indispensable to promote conjugate additions. The adducts made from acids and enone palladium complexes, possibly having an enhanced susceptibility of Pd atom to transmetalation, seem to be intermediates in Lewis acid-promoted palladium-catalyzed conjugate addition. Indeed, we found that **1a** reacted with NaBPh₄ slowly to give the conjugate addition product (eq 5), while neither Pd(PhCH=CHCOCH₃)(PPh₃)₂ (without BF₃) nor PhCH=CHCOCH₃/BF₃ (without Pd) reacted with NaBPh₄, which is also consistent with the results of the MO calculation.



Catalytic Conjugate Addition of Methylaluminum Compounds. The complex **1f** underwent slow decomposition to give the conjugate addition compound PhCH(CH₃)CH₂COCH₃ (18 h, 26%) in benzene, probably through an η^3 -allyl(methyl)-palladium intermediate (eq 6).¹⁰ Although this result suggests

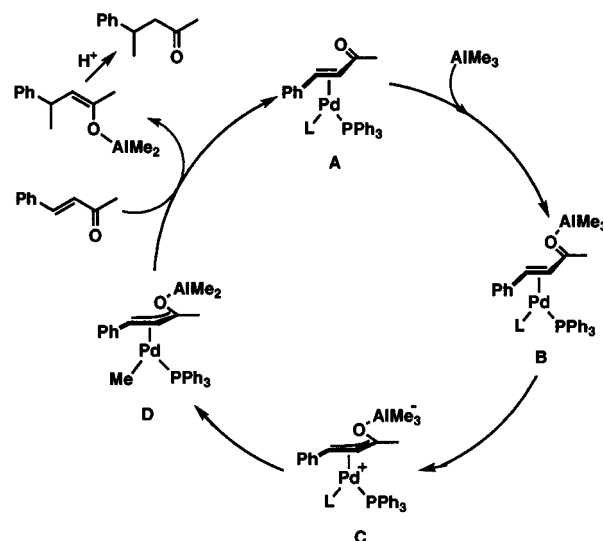


a possibility of catalytic conjugate addition of PhCH=CHCOCH₃ with AlMe₃, the noncatalytic reaction involving these two, which gives rise to the 1,2-addition product PhCH=CHCOH(CH₃)₂ predominantly, was much faster (2 h, 50%) than the catalytic conjugate addition in benzene. Thus, suppression of the 1,2-addition and acceleration of the conjugate addition are required. To suppress the 1,2-addition, the reaction was carried out in THF, in which the 1,2-addition of AlMe₃ did not occur.^{1a} The spectral observation of **1f** having a considerable lifetime suggests that the generation of the η^3 -allyl(methyl)-palladium intermediate from **1f** by transmetalation is slow, possibly due to coordination of two PPh₃ ligands. Thus, to make the transmetalation more feasible, we employed Pd(PPh₃) as a catalyst, which was generated from Pd₂(dba)₃ and 2 equiv of PPh₃ in situ. With this catalyst system, the conjugate addition of AlMe₃ to PhCH=CHCOCH₃ in THF at room temperature occurred quantitatively to give the corresponding product (eq

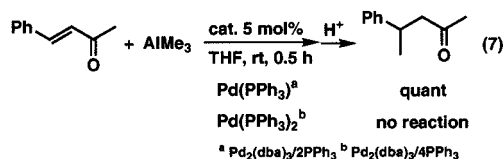
(9) Sakaki, S.; Takeuchi, K.; Sugimoto, M.; Kurosawa, H. *Organometallics* **1997**, *16*, 2995. Kurosawa, H.; Hirako, K.; Natsume, S.; Ogoshi, S.; Kanehisa, N.; Kai, Y.; Sakaki, S.; Takeuchi, K. *Organometallics* **1996**, *15*, 2089.

(10) Palladium-catalyzed conjugate addition of AlR₃ or ZnR₂ has not been reported yet.

Scheme 6. A Plausible Mechanism



7). Both AlEt₃ and ZnEt₂ also underwent conjugate addition under similar conditions.⁹ When Pd(PPh₃)₂ generated from Pd₂(dba)₃ and 4 equiv of PPh₃ was employed as a catalyst, no conjugate addition product was detected under the same conditions.



A possible reaction path is depicted in Scheme 6 (L = solvent or olefins). Coordination of AlMe₃ leads to formation of the intermediate **B**, similar to **1f**, followed by transmetalation to give the η^3 -allyl(methyl)palladium intermediate **D**. Reductive elimination from **D** and subsequent coordination of enone and L regenerate the η^2 -enone complex **A**.

Conclusion

We demonstrated the formation of a new class of complexes showing a wide variety of structures with η^2 -type and η^3 -type coordination of the α,β -unsaturated compounds, starting from palladium(0) complex and Lewis acids. Proposed criteria for estimation of the degree of the contribution of the η^3 -coordination mode to the structure are consistent with the results of the X-ray structure analyses. MO calculation on the set of the model complexes reveals why Lewis acids increase the contribution of the η^3 -coordination mode to the η^2 -enone complex. Moreover, these observations are applied to the construction of the palladium-catalyzed catalytic conjugate addition of the alkylmetals. In principle, this method could be widely applicable to numerous combinations of unsaturated compounds, low-valent transition metals, and Lewis acids.

Experimental Section

General. All manipulations were conducted under a nitrogen atmosphere using standard Schlenk or drybox techniques. ¹H, ³¹P, and ¹³C nuclear magnetic resonance spectra were recorded on JEOL GSX-270S and JEOL AL-400 spectrometers. Elemental analyses were performed at the Instrumental Analysis Center, Faculty of Engineering, Osaka University. For some compounds, accurate elemental analyses

were precluded by extreme air or thermal sensitivity and/or systematic problems with elemental analysis of organometallic compounds.¹¹

Materials. Unless indicated otherwise, solvents and reagents were purchased from commercial vendors, distilled, and degassed prior to use. B(C₆F₅)₃ (3.9 wt % PF-3/Isoper E solution) was donated by Asahi Glass Co. Tetrahydrofuran, benzene, and hexane were purified by distillation from sodium benzophenone ketyl. Celite filtrations were performed by using a plug of Hyflo Super Gel (Wako) over glass wool in disposal pipets or alone on glass filters under vacuum.

(PhCHCHCCH₃(OBf₃)Pd(PPh₃)₂ (1a). To a solution of Pd(PhCH=CHCOCH₃)(PPh₃)₂ (116.0 mg, 0.149 mmol) in 5 mL of THF was added 18.9 μL of BF₃·OEt₂ (21.1 mg, 0.149 mmol) at room temperature, and the solution changed from yellow to red. The reaction mixture was concentrated in vacuo to give orange solids (**1a**) quantitatively. The solids were washed with hexane to give 117.3 mg of **1a** in 93% isolated yield. An analytical sample was prepared by recrystallization from THF/hexane solution. ¹H NMR (C₆D₆): δ 1.73 (d, *J*_{HP} = 6.8 Hz, 3H), 4.47 (ddd, *J*_{HH} = 9.7 Hz, *J*_{HP} = 1.8, 6.2 Hz, 1H), 4.98 (ddd, *J*_{HH} = 9.7 Hz, *J*_{HP} = 4.3, 9.5 Hz, 1H), 6.66 (*J*_{HH} = 7.6 Hz, 2H), 6.84–6.91 (m, 21H), 7.19–7.21 (m, 6H), 7.37–7.47 (m, 6H). ³¹P NMR (C₆D₆): δ 24.72 (d, *J*_{PP} = 24.4 Hz), 30.64 (d, *J*_{PP} = 24.4 Hz). ¹³C NMR (C₆D₆): δ_(CO) 191.5. Anal. Calcd for C₄₆H₄₀BF₃OP₂Pd: C, 65.39; H, 4.77. Found: C, 65.83; H, 4.91.

(PhCHCHCCH₃(OB(C₆F₅)₃)Pd(PPh₃)₂ (1b). ¹H NMR (C₆D₆): δ 1.39 (d, *J*_{HP} = 6.8 Hz, 3H), 4.66 (ddd, *J*_{HH} = 10.4 Hz, *J*_{HP} = 2.1, 5.7 Hz, 1H), 5.06 (ddd, *J*_{HH} = 10.4 Hz, *J*_{HP} = 3.6, 8.3 Hz, 1H), 6.63 (d, *J*_{HH} = 6.5 Hz 2H), 6.79–7.01 (m, 6H), 7.18–7.21 (m, 6H). ³¹P NMR (C₆D₆): δ 24.07 (d, *J*_{PP} = 18.4 Hz), 29.53 (d, *J*_{PP} = 18.4 Hz). ¹³C NMR (C₆D₆): δ_(CO) 198.7. Anal. Calcd for C₄₆H₄₀BF₁₅OP₂Pd: C, 59.63; H, 3.13. Found: C, 59.39; H, 3.44. X-ray data for **1b**: *M* = 1332.24, triclinic, space group *P* $\bar{1}$, *a* = 13.4848(6) Å, *b* = 19.7981(7) Å, *c* = 12.5442(6) Å, α = 95.005(5)°, β = 108.253(4)°, γ = 104.492(2)°, *V* = 3028.9(2) Å³, *D*_{calcd} = 1.461 g/cm³, *Z* = 2, *T* = 23.0 °C, *R* (*R*_w) = 0.086 (0.117).

(PhCHCHCCH₃(OAlCl₃)Pd(PPh₃)₂ (1c). ¹H NMR (C₆D₆): δ 1.52 (dd, *J*_{HP} = 2.8, 8.4 Hz, 3H), 4.44 (dd, *J*_{HH} = 10.8 Hz, *J*_{HP} = 4.3 Hz, 1H), 4.99 (ddd, *J*_{HH} = 10.8 Hz, *J*_{HP} = 2.7, 9.7 Hz, 1H), 6.55 (d, *J*_{HH} = 7.2 Hz, 2H), 6.85–7.01 (m, 21H), 7.13–7.16 (m, 6H), 7.27–7.31 (m, 6H). ³¹P NMR (C₆D₆): δ 23.49 (d, *J*_{PP} = 31.8 Hz), 30.25 (d, *J*_{PP} = 31.8 Hz). ¹³C NMR (C₆D₆): δ_(CO) 182.1. X-ray data for **1c**·THF: *M* = 982.62, orange, monoclinic, *P*_{21/n}, *a* = 18.1758(3) Å, *b* = 12.1664(3) Å, *c* = 21.8447(1) Å, β = 93.679(2)°, *V* = 4820.7(1) Å³, *Z* = 4, *D*_{calcd} = 1.354 g/cm³, *T* = 23.0 °C, *R* (*R*_w) = 0.073 (0.108).

(PhCHCHCCH₃(OAlMeCl₂)Pd(PPh₃)₂ (1d). ¹H NMR (C₆D₆): δ 0.15 (s, 3H), 1.58 (dd, *J*_{HP} = 2.4, 7.6 Hz, 3H), 4.49 (ddd, *J*_{HH} = 10.3 Hz, *J*_{HP} = 5.3, 1.4 Hz, 1H), 4.98 (ddd, *J*_{HH} = 10.3 Hz, *J*_{HP} = 3.6, 10.1 Hz, 1H), 6.57 (d, *J*_{HH} = 7.2 Hz, 2H), 6.87–7.00 (m, 21H), 7.15–7.31 (m, 6H), 7.32–7.35 (m, 6H). ³¹P NMR (C₆D₆): δ 24.69 (d, *J*_{PP} = 26.9 Hz), 30.72 (d, *J*_{PP} = 26.9 Hz). ¹³C NMR (C₆D₆): δ_(CO) 188.1. X-ray data for **1d**·THF: *M* = 962.20, red, monoclinic, *P*_{21/n}, *a* = 18.245(2) Å, *b* = 12.104(1) Å, *c* = 21.929(1) Å, β = 94.015(1)°, *V* = 4831.0(7) Å³, *Z* = 4, *D*_{calcd} = 1.323 g/cm³, *T* = 23.0 °C, *R* (*R*_w) = 0.070 (0.075).

(PhCHCHCCH₃(OAlMe₂Cl)Pd(PPh₃)₂ (1e). ¹H NMR (C₆D₆): δ 0.02 (s, 3H), 0.06 (s, 3H), 1.59 (d, *J*_{HP} = 5.6 Hz, 3H), 4.52 (m, 1H), 5.00 (m, 1H), 6.59 (d, *J*_{HH} = 7.0 Hz, 2H), 6.94 (m, 21H), 7.16 (m, 6H), 7.35 (m, 6H). ³¹P NMR (C₆D₆): δ 24.07 (d, *J*_{PP} = 20.8 Hz), 29.28 (d, *J*_{PP} = 20.8 Hz). ¹³C NMR (C₆D₆): δ_(CO) 193.8. X-ray data for **1e**·THF: *M* = 941.78, orange, monoclinic, *P*_{21/n}, *a* = 18.2637(3) Å, *b* = 12.0305(1) Å, *c* = 22.0524(5) Å, β = 93.639(2)°, *V* = 4835.6(1) Å³, *Z* = 4, *D*_{calcd} = 1.294 g/cm³, *T* = 23.0 °C, *R* (*R*_w) = 0.082 (0.113).

(PhCHCHCCH₃(OAlMe₃)Pd(PPh₃)₂ (1f). To a solution of Pd(PhCH=CHCOCH₃)(PPh₃)₂ (100.8 mg 0.13 mmol) in THF (5 mL) was added 0.13 mL (1.01 M) of a solution of AlMe₃ in hexane, and the reaction mixture changed to orange. The reaction mixture was concentrated, and the residue was washed with hexane to give yellow solids quantitatively. Recrystallization failed due to the decomposition to give the corresponding conjugate addition product (18 h, 26%). ¹H NMR (C₆D₆): δ 0.03 (s, 9H), 1.52 (d, *J*_{HP} = 4.6 Hz, 3H), 4.55 (ddd,

*J*_{HH} = 9.5 Hz, *J*_{HP} = 2.4, 6.5 Hz, 1H), 5.07 (ddd, *J*_{HH} = 9.5 Hz, *J*_{HP} = 5.3, 8.8 Hz, 1H), 6.60 (d, *J*_{HH} = 6.5 Hz, 2H), 6.93 (m, 21H), 7.16 (m, 6H), 7.32–7.37 (m, 6H). ³¹P NMR (C₆D₆): δ 24.59 (d, *J*_{PP} = 13.5 Hz), 28.58 (d, *J*_{PP} = 13.5 Hz).

(CH₂CHCCH₃(OBf₃)Pd(PPh₃)₂ (2a). To a solution of Pd(CH₂=CHCOCH₃)(PPh₃)₂ (100.4 mg, 0.143 mmol) in 5 mL of THF was added 18.0 μL of BF₃·OEt₂ (16.1 mg, 0.142 mmol) at room temperature. The reaction mixture was concentrated in vacuo to give yellow solids quantitatively. The solids were washed with hexane and recrystallized from THF/hexane solution to give orange solids (60.1 mg, 55%). ¹H NMR (C₆D₆): δ 1.63 (d, *J*_{HP} = 8.4 Hz, 3H), 2.29 (dt, *J*_{HH} = 2.6, 10.2 Hz, *J*_{HP} = 7.6 Hz, 1H), 3.55 (dddd, *J*_{HH} = 2.6, 7.5 Hz, *J*_{HP} = 4.9, 11.1 Hz, 1H), 3.97 (ddd, *J*_{HH} = 7.5, 10.2 Hz, *J*_{HP} = 7.7 Hz, 2H), 6.90–7.41 (m, 30H). ³¹P NMR (C₆D₆): δ 22.92 (d, *J*_{PP} = 19.5 Hz), 36.02 (d, *J*_{PP} = 19.5 Hz). ¹³C NMR (CDCl₃): δ_(CO) 187.2. Anal. Calcd for C₄₀H₃₆BF₃OP₂Pd: C, 62.48; H, 4.72. Found: C, 62.73; H, 4.88.

(CH₂CHCCH₃(OB(C₆F₅)₃)Pd(PPh₃)₂ (2b). To a solution of Pd(CH₂=CHCOCH₃)(PPh₃)₂ (195.3 mg, 0.278 mmol) in 5 mL of THF was added 5.0 mL of B(C₆F₅)₃ (142.0 mg, 0.277 mmol) at room temperature, and the solution changed from yellow to orange. The reaction mixture was concentrated in vacuo to give yellow solids quantitatively. The solids were washed with hexane and recrystallized from THF/hexane solution to give yellow solids (187.9 mg, 56%). ¹H NMR (C₆D₆): δ 1.12 (d, *J*_{HP} = 8.8 Hz, 3H), 2.41 (ddd, *J*_{HH} = 3.0, 10.2 Hz, *J*_{HP} = 7.7 Hz, 1H), 3.45 (ddd, *J*_{HH} = 3.0, 6.7 Hz, *J*_{HP} = 10.8 Hz, 1H), 4.11 (ddd, *J*_{HH} = 6.7, 10.2 Hz, *J*_{HP} = 6.5 Hz, 1H), 6.78–7.20 (m, 30H). ³¹P NMR (C₆D₆): δ 23.64 (d, *J*_{PP} = 15.3 Hz), 34.24 (d, *J*_{PP} = 15.3 Hz). ¹³C NMR (C₆D₆): δ_(CO) 198.2. Anal. Calcd for C₃₈H₃₆BF₁₅OP₂Pd: C, 57.43; H, 2.99. Found: C, 57.67; H, 3.27.

(PhCHCHCH(OBf₃)Pd(PPh₃)₂ (3a). ¹H NMR (C₆D₆): δ 4.63 (ddd, *J*_{HH} = 3.3, 10.9 Hz, *J*_{HP} = 3.3 Hz, 1H), 5.01 (ddd, *J*_{HH} = 10.9 Hz, *J*_{HP} = 2.9, 10.9 Hz, 1H), 6.53 (d, *J*_{HH} = 7.2 Hz, 2H), 6.79–6.95 (m, 21H), 7.04–7.10 (m, 6H), 7.45–7.50 (m, 6H), 7.88 (dd, *J*_{HH} = 3.3 Hz, *J*_{HP} = 5.2 Hz, 1H). ³¹P NMR (C₆D₆): δ 24.41 (d, *J*_{PP} = 37.4 Hz), 29.01 (d, *J*_{PP} = 37.4 Hz). ¹³C NMR (C₆D₆): δ_(CO) 157.6. Anal. Calcd for C₄₅H₃₈BF₃OP₂Pd: C, 65.04; H, 4.61. Found: C, 64.65; H, 4.82. X-ray data for **3a**·THF: *M* = 891.04, triclinic, space group *P* $\bar{1}$, *a* = 17.952(10) Å, *b* = 18.473(4) Å, *c* = 12.912(2) Å, α = 89.89(2)°, β = 89.99(3)°, γ = 90.46(3)°, *V* = 4283(2) Å³, *D*_{calcd} = 1.382 g/cm³, *Z* = 4, *T* = 15.0 °C, *R* (*R*_w) = 0.083 (0.116).

(PhCHCHCH(OB(C₆F₅)₃)Pd(PPh₃)₂ (3b/3b'') = 26/1). 3b. ¹H NMR (C₆D₆): δ 4.92 (ddd, *J*_{HH} = 3.7, 10.8 Hz, *J*_{HP} = 3.7 Hz, 1H), 5.32 (ddd, *J*_{HH} = 10.8 Hz, *J*_{HP} = 1.8, 10.8 Hz, 1H), 6.55 (d, *J*_{HH} = 7.2 Hz, 2H), 6.72–6.89 (m, 6H), 6.90–6.92 (m, 12H), 6.99–7.06 (m, 12H), 7.69 (brs, 1H). ³¹P NMR (C₆D₆): δ 23.04 (d, *J*_{PP} = 30.5 Hz), 27.93 (d, *J*_{PP} = 30.5 Hz). ¹³C NMR (C₆D₆): δ_(CO) 166.0.

3b'. ¹H NMR (C₆D₆): δ 3.72 (d, *J*_{HH} = 10.2 Hz, 1H), 5.56 (dd, *J*_{HH} = 10.8 Hz, *J*_{HP} = 10.8 Hz, 1H), 6.41 (d, *J*_{HH} = 7.2 Hz, 2H), 6.72 (t, 7.0 Hz, 3H), 8.02 (d, *J*_{HH} = 4.0 Hz, 1H). The other resonances are hidden by those of the major isomer. Anal. Calcd for C₆₃H₃₈BF₁₅OP₂Pd: C, 59.34; H, 3.00. Found: C, 58.98; H, 3.37. X-ray data for **3b'**·THF: *M* = 1347.23, red, triclinic, *P* $\bar{1}$, *a* = 14.2626(6) Å, *b* = 18.8457(9) Å, *c* = 13.5537(2) Å, α = 105.384(2)°, β = 118.213(3)°, γ = 93.552(2)°, *V* = 3019.0(2) Å³, *Z* = 2, *D*_{calcd} = 1.482 g/cm³, *T* = 23.0 °C, *R* (*R*_w) = 0.077 (0.112).

(CH₂CHCH(OBf₃)Pd(PPh₃)₂ (4a). ¹H NMR (C₆D₆): δ 2.60 (ddd, *J*_{HH} = 2.9, 6.9 Hz, *J*_{HP} = 6.9 Hz, 1H), 3.46 (ddd, *J*_{HH} = 2.9, 10.2 Hz, *J*_{HP} = 6.9 Hz, 1H), 4.07 (ddd, *J*_{HH} = 2.9, 6.9, 10.2 Hz, 1H), 7.00–7.08 (m, 18H), 7.36–7.48 (m, 12H), 7.90 (dd, *J*_{HH} = 2.9 Hz, *J*_{HP} = 5.9 Hz, 1H). ³¹P NMR (C₆D₆): δ 21.70 (d, *J*_{PP} = 29.4 Hz), 34.68 (d, *J*_{PP} = 29.4 Hz). ¹³C NMR (C₆D₆): δ_(CO) 161.5. Anal. Calcd for C₃₉H₃₄BF₃OP₂Pd: C, 62.05; H, 4.54. Found: C, 61.67; H, 4.69. X-ray data for **4a**: *M* = 754.85, yellow, monoclinic, *P*_{21/c}, *a* = 17.8836(3) Å, *b* = 11.4747(2) Å, *c* = 18.263(1) Å, β = 106.656(2)°, *V* = 3590.5(2) Å³, *Z* = 4, *D*_{calcd} = 1.396 g/cm³, *T* = 23.0 °C, *R* (*R*_w) = 0.073 (0.074).

(CH₂CHCH(OB(C₆F₅)₃)Pd(PPh₃)₂ (4b). ¹H NMR (C₆D₆): δ 2.72 (ddt, *J* = 2.3, 7.5 Hz, *J*_{HP} = 6.1 Hz, 1H), 3.50 (ddt, *J* = 2.3, 11.1 Hz, *J*_{HP} = 8.5 Hz, 1H), 4.26 (ddd, *J* = 3.8, 7.5, 11.1 Hz, 1H), 6.85–6.99 (m, 18H), 7.06–7.10 (m, 6H), 7.29–7.34 (m, 6H), 7.70 (d, *J* = 3.8 Hz, *J*_{HP} = 5.6 Hz, 1H). ³¹P NMR (C₆D₆): δ 21.99 (d, *J*_{PP} = 25.7 Hz),

(11) See the Supporting Information in the following: Carney, M. J.; Walsh, P. J.; Bergman, R. G. *J. Am. Chem. Soc.* **1990**, *112*, 6426.

33.10 (d, $J_{PP} = 25.7$ Hz). ^{13}C NMR (C_6D_6): $\delta_{(\text{CO})}$ 169.7. Anal. Calcd for $\text{C}_{57}\text{H}_{34}\text{BF}_{15}\text{OP}_2\text{Pd}$: C, 57.10; H, 2.86. Found: C, 57.12; H, 3.09. Crystal data for **4b**: $M = 1199.03$, yellow, triclinic, $P\bar{1}$ (No. 2), $a = 14.555(3)$ Å, $b = 17.376(4)$ Å, $c = 10.860(4)$ Å, $\alpha = 97.73(3)^\circ$, $\beta = 103.05(2)^\circ$, $\gamma = 105.88(2)^\circ$, $V = 2516(1)$ Å³, $Z = 4$, $D_{\text{calcd}} = 3.164$ g/cm³, $T = 23.0$ °C, R (R_w) = 0.045 (0.039).

[(η^3 -PhCHCH₂)Pd(PPh₃)₂][BF₄]. ^1H NMR (400 MHz, C_6D_6): δ 3.64 (ddd, $J_{\text{HH}} = 6.6$, 0.5 Hz, $J_{\text{HP}} = 6.6$ Hz, 1H), 3.96 (ddd, $J_{\text{HH}} = 11.5$, 1.0 Hz, $J_{\text{HP}} = 11.5$ Hz, 1H), 5.85 (dddd, $J_{\text{HH}} = 11.5$, 1.0, 0.5 Hz, $J_{\text{HP}} = 11.9$ Hz, 1H), 6.59 (m, 4H), 6.63 (m, 1H), 6.91–7.24 (m, 7H), 7.02 (m, 6H), 7.08 (m, 6H), 7.22 (m, 6H), 7.54 (m, 6H). ^{31}P NMR (109 MHz, C_6D_6): δ 25.43 (d, $J_{\text{PP}} = 46.5$ Hz), 27.07 (d, $J_{\text{PP}} = 46.5$ Hz). Anal. Calcd for $\text{C}_{45}\text{H}_{39}\text{BF}_4\text{P}_2\text{Pd}$: C, 64.73; H, 4.41. Found: C, 65.00; H, 4.73.

Pd(PhCH=CHCOCH₃)(dppf). A solution of (η^3 -CH₂CHCH₂)PdCp (202.0 mg, 0.946 mmol), PhCH=COCH₃ (136.9 mg, 0.936 mmol), and DPPF (520.4 mg, 0.939 mmol) in 15 mL of THF was stirred for 2 h at room temperature. The reaction mixture was concentrated in vacuo and washed with hexane to give yellow solids (629.6 mg, 83%). ^1H NMR (C_6D_6): δ 1.76 (s, 3H), 3.78 (brs, 2H), 3.85 (brs, 1H), 3.96 (brs, 1H), 4.01 (brs, 1H), 4.08 (brs, 2H), 4.48 (brs, 1H), 5.01 (ddd, $J_{\text{HH}} = 10.8$ Hz, $J_{\text{HP}} = 4.1$, 7.3 Hz, 1H), 5.34 (dd, $J_{\text{HH}} = 10.8$ Hz, $J_{\text{HP}} = 7.3$ Hz, 1H), 6.88–7.22 (m, 19H), 7.64 (m, 2H), 7.86 (m, 4H). ^{31}P NMR (C_6D_6): δ 18.58 (s), 18.62 (s).

(PhCHCHCCH₃(OBf₃))Pd(dppf) (5a). To a solution of Pd(PhCH=CHCOCH₃)(dppf) (103.5 mg, 0.128 mmol) in 3 mL of THF was added 16.2 μL of BF₃·OEt₂ (18.1 mg, 0.128 mmol) at room temperature, and the solution changed from orange to red. The reaction mixture was concentrated in vacuo to give yellow solids quantitatively. The solids were washed with hexane and recrystallized from THF/hexane solution to give yellow solids (7.1 mg, 6%). ^1H NMR (C_6D_6): δ 1.69 (dd, $J_{\text{HP}} = 3.4$, 8.2 Hz, 3H), 3.56 (brs, 2H), 3.66 (brs, 1H), 3.81 (m, 2H), 3.95 (brs, 1H), 4.25 (brs, 1H), 4.58 (dd, $J_{\text{HH}} = 10.3$ Hz, $J_{\text{HP}} = 6.2$ Hz, 1H), 4.77 (ddd, $J_{\text{HH}} = 10.3$ Hz, $J_{\text{HP}} = 2.4$, 9.7 Hz, 1H), 5.62 (brs, 1H), 6.69 (d, $J_{\text{HH}} = 5.4$ Hz, 2H), 6.73–7.08 (m, 15H), 7.35 (m, 2H), 7.55 (m, 2H), 7.70 (m, 2H), 7.92 (m, 2H). ^{31}P NMR (C_6D_6): δ 22.34 (d, $J_{\text{PP}} = 45.9$ Hz), 25.27 (d, $J_{\text{PP}} = 45.9$ Hz).

(PhCHCHCCH₃(OB(C₆F₅)₃))Pd(dppf) (5b). To a solution of Pd(PhCH=CHCOCH₃)(dppf) (102.3 mg, 0.127 mmol) in 3 mL of THF was added 2.2 mL of B(C₆F₅)₃ (62.5 mg, 0.122 mmol) at room temperature, and the solution changed from orange to red. The reaction mixture was concentrated in vacuo to give orange solids quantitatively. The solids were washed with hexane and recrystallized from THF/hexane solution to give orange crystals (58.4 mg, 35%). ^1H NMR (C_6D_6): δ 1.17 (dd, $J_{\text{HP}} = 1.9$, 7.8 Hz, 3H), 3.61 (brs, 1H), 3.68 (brs, 1H), 3.72 (brs, 1H), 3.77 (brs, 3H), 4.29 (brs, 1H), 4.81 (brs, 1H), 4.89 (brs, 1H), 4.89 (m, 2H), 6.78–7.03 (m, 20H), 7.58–7.74 (m, 5H). ^{31}P NMR (C_6D_6): δ 20.78 (d, $J_{\text{PP}} = 41.9$ Hz), 25.80 (d, $J_{\text{PP}} = 41.9$ Hz). Crystal data for **5b**: $M = 1330.97$, orange, triclinic, $P\bar{1}$ (No. 2), $a = 14.0407(8)$ Å, $b = 16.7253(8)$ Å, $c = 13.5783(9)$ Å, $\alpha = 11.592(4)^\circ$, $\beta = 112.023(2)^\circ$, $\gamma = 76.314(3)^\circ$, $V = 2730.5(3)$ Å³, $Z = 2$, $D_{\text{calcd}} = 1.619$ g/cm³, $T = 23.0$ °C, R (R_w) = 0.066 (0.076).

(PhCHCHCCH₃(OAlCl₃))Pd(dppf) (5c). To a solution of Pd(PhCH=CHCOCH₃)(dppf) (151.6 mg, 0.188 mmol) in 3 mL of THF was added AlCl₃ (26.1 mg, 0.196 mmol) at room temperature, and the solution changed from orange to red. The reaction mixture was concentrated in vacuo to give yellow solids quantitatively. The solids were washed with hexane and recrystallized from THF/hexane solution to give red crystals (50.1 mg, 28%). ^1H NMR (C_6D_6): δ 1.51 (dd, $J_{\text{HP}} = 4.1$, 9.2 Hz, 3H), 3.56 (d, $J_{\text{HH}} = 6.8$ Hz, 1H), 3.81 (d, $J_{\text{HH}} = 6.2$ Hz, 1H), 4.04 (brs, 1H), 4.35 (brs, 1H), 4.58 (m, 1H), 4.77 (m, 1H), 5.07 (brs, 1H), 6.46 (d, $J_{\text{HH}} = 7.5$ Hz, 2H), 6.54–7.03 (m, 12H), 7.11–7.25 (m, 4H), 7.37–7.45 (m, 4H), 7.55–7.72 (m, 3H). ^{31}P NMR (C_6D_6): δ 21.28 (d, $J_{\text{PP}} = 51.1$ Hz), 25.88 (d, $J_{\text{PP}} = 51.1$ Hz). Anal. Calcd for $\text{C}_{44}\text{H}_{38}\text{AlCl}_3\text{OP}_2\text{FePd}$: C, 56.20; H, 4.07. Found: C, 55.52; H, 4.51. Crystal data for **5c**·THF: $M = 1012.43$, red, triclinic, $P\bar{1}$ (No. 2), $a = 17.890(2)$ Å, $b = 221.853(2)$ Å, $c = 12.076(1)$ Å, $\alpha = 90.103(2)^\circ$, $\beta = 90.145(1)^\circ$, $\gamma = 93.822(3)^\circ$, $V = 4710.6(8)$ Å³, $Z = 5$, $D_{\text{calcd}} = 1.784$ g/cm³, $T = 23.0$ °C, R (R_w) = 0.088 (0.129).

Pd(PhCH=CHCHO)(dppf). To a solution of (η^3 -CH₂CHCH₂)PdCp (201.3 mg, 0.942 mmol) and dppf (519.9 mg, 0.938 mmol) in 15 mL of THF was added 0.12 mL of PhCH=CHCHO (125.8 mg, 0.952 mmol), the mixture was stirred for 2 h at room temperature, and the solution changed from red to orange. The reaction mixture was concentrated in vacuo and washed with hexane to give yellow solids quantitatively (617.0 mg, 83%). ^1H NMR (C_6D_6): δ 3.86 (m, 5H), 4.24 (m, 3H), 5.06 (m, 2H), 6.84–7.16 (m, 19H), 7.74 (m, 4H), 7.95 (m, 2H) 9.35 (d, $J_{\text{HH}} = 5.4$ Hz). ^{31}P NMR (C_6D_6): δ 25.49 (s).

(PhCHCHCH(OBF₃))Pd(dppf) (6a). To a solution of Pd(PhCH=CHCHO)(dppf) (100.0 mg, 0.126 mmol) in 10 mL of THF was added 16.0 μL of BF₃·OEt₂ (17.9 mg, 0.126 mmol) at room temperature, and the solution changed from yellow to orange. The reaction mixture was concentrated in vacuo to give yellow solids quantitatively. The solids were washed with hexane and recrystallized from THF/hexane solution to give yellow solids (20.7 mg, 19%). ^1H NMR (C_6D_6): δ 3.58 (m, 1H), 3.66 (m, 2H), 3.81 (m, 1H), 3.87 (m, 1H), 3.90 (m, 1H), 4.65 (m, 1H), 4.93 (m, 1H), 5.71 (m, 1H), 6.64 (m, 2H), 6.80–7.21 (m, 13H), 7.73 (m, 2H), 7.50 (m, 3H), 7.66 (m, 2H), 7.78 (m, 1H), 7.90 (m, 2H). ^{31}P NMR (C_6D_6): δ 21.82 (d, $J_{\text{PP}} = 54.4$ Hz), 25.66 (d, $J_{\text{PP}} = 54.4$ Hz).

(PhCHCHCH(OB(C₆F₅)₃))Pd(dppf) (6b). To a solution of Pd(PhCH=CHCHO)(dppf) (100.2 mg, 0.126 mmol) in 11 mL of THF was added 2.3 mL of B(C₆F₅)₃ (65.3 mg, 0.128 mmol) at room temperature, and the solution changed from yellow to red. The reaction mixture was concentrated in vacuo to give orange solids quantitatively. The solids were washed with hexane and recrystallized from THF/hexane solution to give orange solids. ^1H NMR (C_6D_6): δ 3.66 (brs, 3H), 3.81 (brs, 3H), 3.89 (brs, 2H), 4.06 (brs, 1H), 4.69 (brs, 1H), 4.93 (ddd, $J_{\text{HH}} = 4.1$, 11.3 Hz, $J_{\text{HP}} = 4.1$ Hz, 1H), 5.31 (dd, $J_{\text{HH}} = 11.3$ Hz, $J_{\text{HP}} = 11.3$ Hz, 1H), 6.72–7.26 (m, 20H), 7.50 (m, 2H), 7.62 (m, 1H), 7.74 (m, 2H), 7.83 (brs, 1H). ^{31}P NMR (C_6D_6): δ 20.61 (d, $J_{\text{PP}} = 51.4$ Hz), 27.65 (d, $J_{\text{PP}} = 51.4$ Hz). Anal. Calcd for $\text{C}_{61}\text{H}_{36}\text{BF}_{15}\text{OP}_2\text{FePd}$: C, 56.15; H, 2.78. Found: C, 55.84; H, 3.06.

Reaction of 1a with NaBPh₄. **1a** (15.6 mg, 0.0185 mmol) and NaBPh₄ (7.2 mg, 0.0210 mmol) were placed in a sealed NMR tube, and C_6D_6 (0.6 mL) was added. The sample was heated at 80 °C and followed by ^1H NMR. Selected spectral data for Ph₂CHCH₂COCH₃ are given here. ^1H NMR (C_6D_6): δ 1.55 (s, 3H), 2.69 (d, $J_{\text{HH}} = 7.43$ Hz, 2H), 4.62 (t, $J_{\text{HH}} = 7.43$ Hz, 1H).

MO Calculation. Molecular geometry optimization followed by analytical frequency calculations was performed at the B3LYP/BS-1 (BS-1: Pd, valence electrons (5s 5p 4d)/[3s 3p 2d], core electrons ECPs (up to 3d);¹² P, valence electrons (3s 3p)/[2s 2p], core electrons ECPs (up to 2p);¹³ others, 6-31G*) levels of theory using the Gaussian 94 programs.¹⁴ The ab initio MO/MP2 calculation using BS-2 (BS-2: Pd, valence electrons (5s 5p 4d)/[3s 3p 2d], core electrons ECPs (up to 3d); others, 6-31G*) was carried out on the optimized geometry.

Typical Procedure for Catalytic Reaction (Reaction with AlMe₃). Under a nitrogen atmosphere, to a solution of 146.2 mg of PhCH=CHCOCH₃ (1.0 mmol), 166.7 mg of *n*-nonadecane (internal standard), and 13.1 mg of Pd₂(dba)₃·CHCl₃ in 5.0 mL of THF was added 1.0 mL of a hexane solution of AlMe₃ (1.01 M) at room temperature. The reaction mixture was stirred for 0.5 h and then poured into 5 mL of 1 M HCl aqueous solution. The organic layer was extracted with three portions of 3 mL of Et₂O. The yield was determined by GC. PhCH(CH₃)CHCOCH₃ was obtained quantitatively.

Reaction with AlEt₃. Ten mol % of Pd(PPh₃) was employed. PhCH(CH₂CH₃)CHCOCH₃ was obtained in 72% yield.

(12) Hay, P. J.; Wadt, W. R. *J. Chem. Phys.* **1985**, *82*, 299.

(13) Wadt, W. R.; Hay, P. J. *J. Chem. Phys.* **1985**, *82*, 284.

(14) Frisch, M. J.; Trucks, G. W.; Schlegel, H. B.; Gill, P. M. W.; Johnson, B. G.; Robb, M. A.; Cheeseman, J. R.; Keith, T. A.; Petersson, G. A.; Montgomery, J. A.; Raghavachari, K.; Al-Laham, M. A.; Zakrzewski, V. G.; Oritiz, J. V.; Foresman, J. B.; Cioslowski, J.; Stefanov, B. B.; Nanayakkara, A.; Chalacombe, M.; Peng, C. Y.; Ayala, P. Y.; Chen, W.; Wong, M. W.; Andres, J. L.; Replogle, E. S.; Gomperts, R.; Martin, R. L.; Fox, D. J.; Binkley, J. S.; Defrees, D. J.; Baker, J.; Stewart, J. P.; Head-Gordon, M.; Gonzalez, C.; People, J. A. *Gaussian 94*; Gaussian, Inc.: Pittsburgh, PA, 1995.

Reaction with ZnEt₂. Ten mol % of Pd(PPh₃) was employed, and the reaction mixture was stirred for 1 h. PhCH(CH₂CH₃)CHCOCH₃ was obtained in 93% yield.

Acknowledgment. Partial support of this work through CREST of the Japan Science and Technology Corporation and Grants-in-Aid for Scientific Research from the Ministry of Education, Science and Culture, Japan, is gratefully acknowledged. We also acknowledge Asahi Glass Co. for the donation of B(C₆F₅)₃.

Supporting Information Available: Details of crystallographic analyses for **1b–e**, **3a**, **3b'**, **4a**, **4b**, **5b**, and **5c**; complete tables of atomic coordinates and selected bond distances and angles for the compounds listed above (PDF). This material is available free of charge via the Internet at <http://pubs.acs.org>.

JA0036099